High Magnetic Field X-ray Magnetic Circular Dichroism- a New Microscopic Magnetization Probe for Any Magnet

A novel tool to evaluate a site and element selective magnetic moment has been developed by combining synchrotron radiation and high magnetic fields. X-ray magnetic circular dichrosim: XMCD is a key method for spintronics materials, however, had been limited in ferromagnets. The present technique breaks this limitation and realizes the "XMCD for any magnet".

A synchrotron X-ray is a powerful tool to investigate materials for the strong intensity and the tunability in X-ray regime. These features make it possible to perform the various types of spectroscopy such as X-ray absorption (XAS) and XMCD. These methods are unique because of element and site selective microscopic probing. For example, XMCD has been established as the microscopic magnetization probe for magnetic materials. One of the most crucial limits of XMCD is that the method can be used only for ferromagnets. To widen the application of XMCD, we have developed a high magnetic field XMCD. The idea is very simple and is straightforward. In a very strong magnetic field, a substantial magnetic moment is induced in any magnet and thus XMCD can be measured in most of magnetic materials.

Figure 1 shows the mini magnetic field generator used for XMCD experiment up to 40 T. Thanks to the extremely small size, the magnet and the capacitor bank are portable and thus the combination with X-ray spectrometer is easy. In fact, the capacitor bank is as small as a small refrigerator and the storing energy is only 10 kJ. Even such small system, a high magnetic field up to 40 T can be achieved.

The first experiment is made for the $EuNi_2(Si_{0.18}Ge_{0.82})_2$, which shows the magnetic field induced valence state transition. It is non-magnetic at zero field and the magnetic interaction is antiferromagnetic. Thus a conventional XMCD cannot be applied for this material. Because of the very strong magnetic field of our instrument, the substantial magnetic moment is induced and the clear MCD signals are observed. It is the first XMCD experiment up to 40 T.

By analyzing the XMCD spectra, we can deduce the polarizations of rare earth element at different component such as 4f and 5d. Also the important parameters such as inter-band mixing and exchange couplings can be also evaluated. These facts show that the method is very unique in the field of magnetism.

By using the high magnetic field, XMCD can be measured many of antiferromagnet and paramagnet. It would open the new field for X-ray spectroscopy.

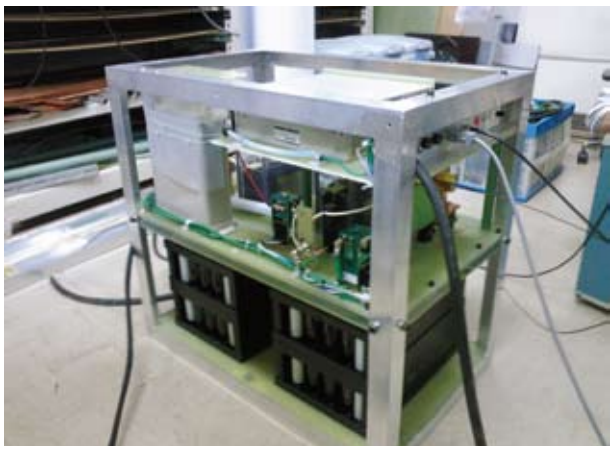

Fig. 1 A pulsed magnetic field generator XMCD. A magnetic field as high as 40 T can be generated.

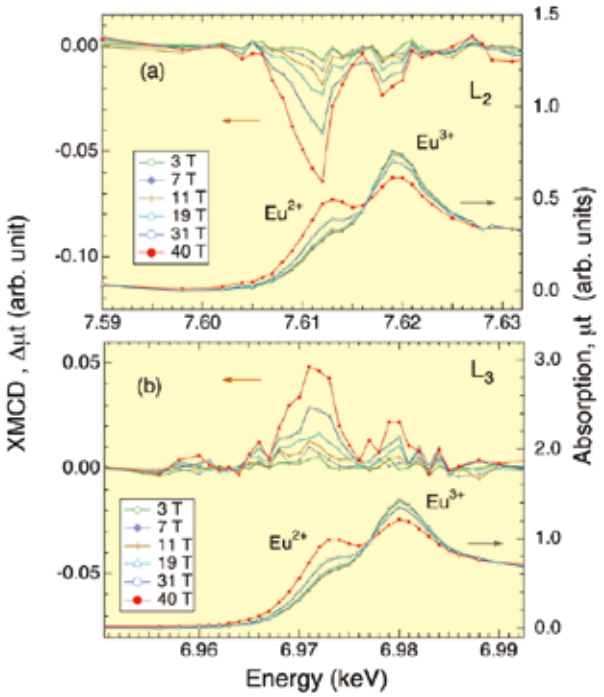

Fig. 2 XMCD spectra of Eu intermetallic compound at L_2 and L_3 edges. The signals grow as a function of magnetic field intensity [1].

References

[1] Y. H. Matsuda, Z. W. Ouyang, H. Nojiri, T. Inami, K. Ohwada, M. Suzuki, N. Kawamura, A. Mitsuda and H. Wada, Phys Reu. Lett. (in print)

Key Words

High Magnetic Field, XMCD, Magnetism

Contact to
Hiroyuki Nojiri (Magnetism Division)
e-mail: nojiri@imr.tohoku.ac.jp

Infrared Optical Probe of Carrier-Doping in Organic Mott Insulator

Modulation of the band-filling in the Mott insulator could produce the novel interesting strongly correlated electronic states. X-ray irradiation for the molecular materials could be a new way of the carrier-doping into the Mott insulators. We can obtain rich information about the correlated states from the Infrared optical properties

Organic charge transfer salts based on the BEDT-TTF molecule have been recognized as one of the highly correlated electron system. Among them, κ- (BEDT-TTF) $_2X$ with X = Cu (NCS) $_2$, Cu[N (CN) $_2$]Y (Y = Br and Cl), etc. have attracted considerable attention from the point of view of the strongly correlated electron system. The strong BEDT-TTF dimer structure makes the conduction band effectively half-filling. In such strongly correlated electron systems, Mott insulating phase appears and the first order Mott insulator – metal transition takes place by applying hydrostatic pressure, which must broaden the conduction bandwidth with respect to the effective Coulomb repulsion energy on the dimer. Thus the κ- (BEDT-TTF) $_2X$ family has been considered to be the bandwidth controlled Mott system in comparison to the filling controlled one in the inorganic perovskites such as High-T_c copper oxides.

X-ray irradiation usually induces disorders in a crystal, for example, displacement of the atomic position. In the case of molecular materials, the irradiation produces molecular defects, which are generated by the radiolysis under ionizing radiation. This kind of molecular defect permanently remains, while the irradiation damage in inorganic materials is only due to atomic displacements which can be restored by a proper heat treatment. These defects and disorders make the electrical conductivity worse in general because of increasing the electron scattering. Increase of the conductivity by x-ray irradiation, however, has been found in organic Mott insulator κ-(BEDT-TTF)$_2$Cu[N(CN)$_2$]Cl [1]. The irradiation-induced defects expected at the donor and/or anion molecule sites might cause a local imbalance of the charge-transfer in the crystal (Figure 1). Such local modulation of the charge-transfer comes into being the effective doping of carriers into the half-filling Mott insulators. In order to investigate the change of the electronic state by possible carrier-doping induced by x-ray irradiation into the organic dimer-Mott insulators, infrared optical reflectivity spectra were measured in typical bandwidth controlled Mott insulator κ-(BEDT-TTF)$_2$Cu[N(CN)$_2$]Cl [2].

In the optical reflectivity spectra (Figure 2) of κ-(BEDT-TTF)$_2$Cu[N(CN)$_2$]Cl after x-ray irradiation by using the tungsten tube (40kV, 20mA), it was apparently observed that the spectral weight was transferred from the high- to low-energy far infrared region. This means that the interband transitions in dimer bands and Hubbard bands in the mid infrared region are suppressed drastically and the low-energy Drude-like part is enhanced by way of compensation. The observed optical spectra suggest that the Mott insulator changes into essentially a metal due to small shift of the carrier number from the half-filling in the conduction band by x-ray irradiation.

As for the future application of this x-ray irradiation technique, a conductive circuit and dots can be made artificially on the molecular crystals by controlling the local irradiated position, which will be useful for fabricating the organic electronic devices [3].

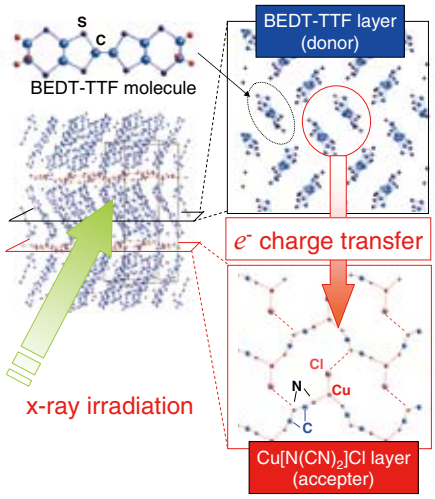

Fig. 1 Crystal structure of κ-(BEDT-TTF)$_2$Cu[N(CN)$_2$]Cl. The two-dimensional conduction plane consists of BEDT-TTF donor molecules, which is sandwiched by the insulating Cu[N(CN)$_2$]Cl anion molecule layers.

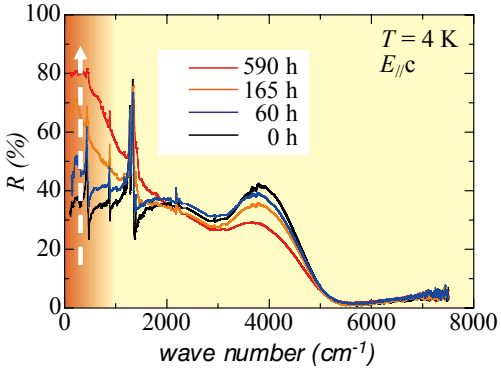

Fig. 2 Optical reflectivity spectra of κ-(BEDT-TTF)$_2$Cu[N(CN)$_2$]Cl at 4 K. Reflectivity in far infrared region increases with increasing the x-ray irradiation time. Concurrently we observe a decrease of the magnitude of the interband transition in the mid infrared region around 3500-4000 cm^{-1}.

References

[1] T. Sasaki, H. Oizumi, N. Yoneyama and N. Kobayashi, J. Phys. Soc. Jpn. **76**, 123701 (2007).

[2] T. Sasaki, N. Yoneyama, Y. Nakamura, N. Kobayashi, Y. Ikemoto, T. Moriwaki and H. Kimura, Phys. Rev. Lett. **101**, 206403 (2008).

[3] N. Yoneyama, T. Sasaki, N. Kobayashi, Y. Ikemoto, T. Moriwaki and H. Kimura, Solid State Commun. **149**, 775 (2009).

Key Words

Organic Conductors, Optical Conductivity, X-ray Irradiation

Contact to

Takahiko Sasaki (Low Temperature Physics Division)

e-mail: takahiko@imr.tohoku.ac.jp

Electric Double Layer Transistor

As an in-house collaboration with Kawasaki-group (WPI-AIMR and IMR) and Nojima-group (IMR), we developed a new electrochemical technique at solid/liquid interfaces. Using the electric double layer as a capacitor, we have fabricated a field effect transistor device, with which we demonstrated electric field induced phase transitions, involving insulator-metal transition and even superconductivity. This transistor can be a versatile method to create and control new states of matter.

The electric double layer formed at an electrochemical interface between liquid and solid is attracting considerable interest from the view point of charge capacitor applications. However, their ability of high density charge accumulation can be used as a transistor with high capacity and high maximum carrier density, which might provide a significant impact on solid state physics.

When voltage is applied between two electrodes in an electrochemical cell, ions in electrolyte move toward corresponding electrodes driven by the electric field. Finally, ions are stabilized right above the electrode surface to form an electric double layer (EDL). Figure 1 shows a schematic drawing of EDL for the case of polymer electrolyte, consisting of polymer solvents and $KClO_4$ solute. EDL is a kind of capacitor, which produces an electric field in the order of 10 MV/cm, which is difficult to achieve in solid capacitors. This capacitor device, called electric double layer capacitor (EDLC) is well known for its capability of high density charge accumulation, and is already on market as a high density and high speed capacitor. When one of the electrodes is replaced by a semiconductor with a source and drain electrodes, this device works as a field effect transistor, which can be called an electric double layer transistor (EDLT). This electrochemical transistor device has been investigated for application to ion sensors or for reducing operation voltages in organic transistors. Since 2005, we have been investigating EDLT devices aiming at accumulating high density carriers and hopefully inducing electronic phase transitions using organic semiconductors [1]. Recently, we started to apply this technique to oxide semiconductors in collaboration with Prof. Kawasaki's group, and have successfully demonstrated the

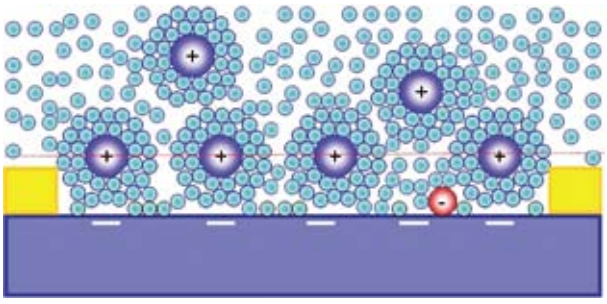

Fig. 1 Schematic drawing of interface between polymer electrolytes and semiconductors under a voltage bias. Solvated cations and accumulated electrons at solid surfaces form an electric double layer with an approximate thickness of 1 nm.

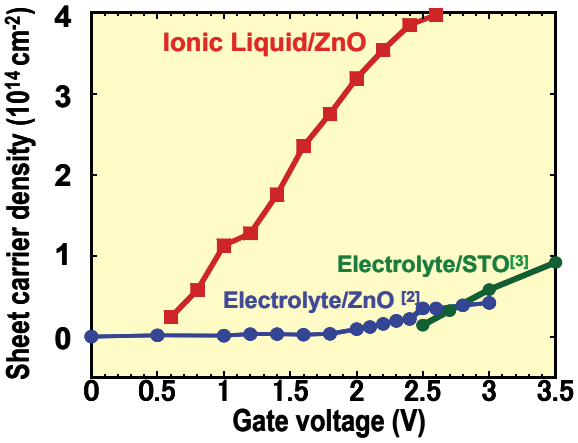

Fig. 2 Gate voltage dependence of carrier density accumulated at EDLT of oxide semiconductor, which was determined by Hall effect measurements. Ionic liquid, specifically DEME-TFSI, displays an significant improvement in carrier density over that for polymer electrolyte.

electric field induced insulator-metal transition in ZnO [2], followed by superconductivity in $SrTiO_3$ [3]. Particularly, the latter is the first electric field induced superconductivity without any help of chemical doping, which has been a target of solid state physicists for about half a century.

For expanding electric field induced phase transitions to other materials, the increase of carrier density is of critical importance. For this purpose, we introduced ionic liquid which is a kind of melt salt at room temperature. Figure 2 displays gate voltage dependence of the carrier density determined by Hall effect measurements on ZnO EDLT devices [4]. The results uncovered that the charge density accumulated with ionic liquid is several times larger than that with polymer electrolyte. The maximum carrier density achieved in Fig. 2 allows us to anticipate to realize electric field induced superconductivity in other materials. These results strongly imply that EDLT could be useful for searching novel states of matter and offers a novel direction in materials research at the electrochemical interface between ionic conductors (generally liquid) and electronic conductors (solid).

Reference

[1] H. Shimotani et al., *Appl. Phys. Lett.* **86**, 022104 (2005).
[2] H. Shimotani et al., *Appl. Phys. Lett.* **91**, 082106 (2007).
[3] K. Ueno et al., *Nat. Mater.* **7**, 855 (2008).
[4] H. T. Yuan et al., *Adv. Funct. Mater.* **19**, 1046 (2009).

Key Words

Field Effect Transistor, Electrochemical Device, Superconductivity

Contact to
Yoshihiro Iwasa (Low Temperature Condensed State Physics Division)
e-mail: iwasa@imr.tohoku.ac.jp

Monolayer Segregation of Dopant Atoms at the Interface between Gate Oxide and Si Substrate in MOSFET Observed by Laser 3D Atom Probe Method

Laser assisted 3D atom probe was applied to analyze three-dimensional dopant distribution in Si substrate of metal-oxide-semiconductor field effect transistor (MOSFET) structure. Monolayer segregation of As atoms at the interface between gate oxide and Si substrate was clearly observed, which is a candidate of the origin of variability in transistor characteristics. This technique is also useful to study degradation of nuclear materials due to impurity segregation on grain boundaries and interfaces.

As the minimum feature size of metal-oxide-semiconductor field effect transistor (MOSFET) decreases to 100 nm or less, variability in MOSFET characteristics has become a serious problem. The major factor is supposed to be random distribution of discrete dopant in the channel region. Therefore, the information on the exact location of each dopant in the channel region is strongly desired. In this work [1], dopant distribution in MOSFET channel was observed with atomic scale resolution using laser-assisted three-dimensional local electrode atom-probe (3DAP) (IMAGO: LEAP3000X).

The sample in this study is laterally uniform and has the dummy structure of MOSFET which consists of polycrystalline Si gate, gate oxide, and Si substrate. After cleaning the surface of Si substrate, As atoms were implanted at the energy of 70 keV with the dose of $2x10^{14}cm^2$. For recovering the implanted damage, a rapid thermal annealing was carried out at 950 °C for 60 s. Next, gate oxide of 2nm thickness and polycrystalline Si gate of 150nm thickness were formed. B atoms were implanted at the energy of 10 keV with the dose of $3x10^{15}cm^2$ for gate pre-doping. Finally, spike annealing for 1050°C was carried out to activate the implanted impurities. The needle sample for 3DAP analysis was prepared using a focused-ion-beam system. The base temperature of the sample during the 3DAP measurement was kept at 30 K.

Figure 1 shows a 3D elemental map of the sample. The box sizes in the figure are $60x60x125nm^3$. 70 nm of the polycrystalline Si layer and 50 nm of the Si substrate across the gate oxide were analyzed. For Si, 5% of atoms are plotted in this figure to make the map clear. The MOSFET structure of the polycrystalline Si gate, the gate oxide, and the Si substrate structure are observed. As atoms implanted in the Si substrate and B atoms implanted in the polycrystalline Si gate were observed.

Figure 2 shows a one-dimensional As atom distribution in the depth direction. The As atom distribution is almost consistent with the result measured by the SIMS in the region of the Si substrate. However, at the interface between the gate oxide and the Si substrate, the As concentration determined by the 3DAP is higher than the SIMS results. This result indicates that the As atoms segregate at the interface. This segregation can be confirmed by the enlarged view of the 3D elemental map around the interface shown in Fig. 3. It is clearly observed that the As atoms are located just at the interface with higher concentration. This monolayer segregation is important to understand the chemical and electrical states of the As atoms in the MOSFET, which may affect threshold voltage, effective mobility, and gate oxide reliability. Moreover, the influence of the segregation will become more serious to the device behavior in further downsizing MOSFETs.

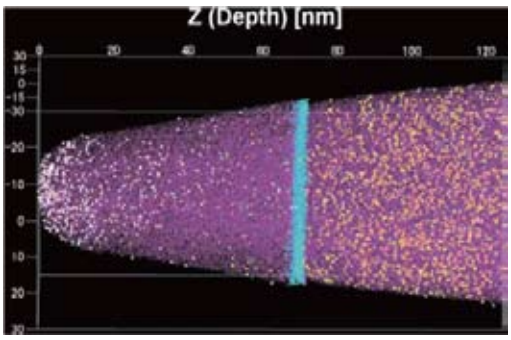

Fig. 1 3D elemental map of the MOSFET structure sample. As (yellow), B (white), O (blue), and Si (magenta). For visual clarity, only 5% of the Si atoms are plotted.

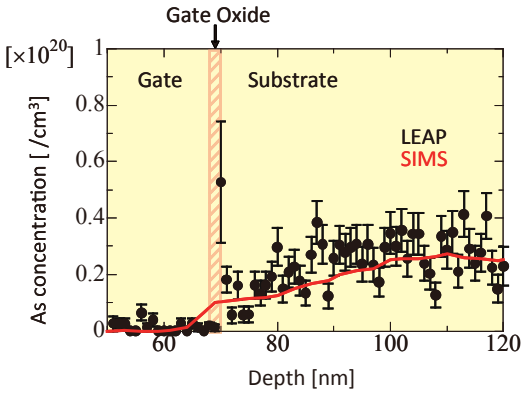

Fig. 2 1D As atom distribution in the depth direction from the 3DAP and SIMS analyses.

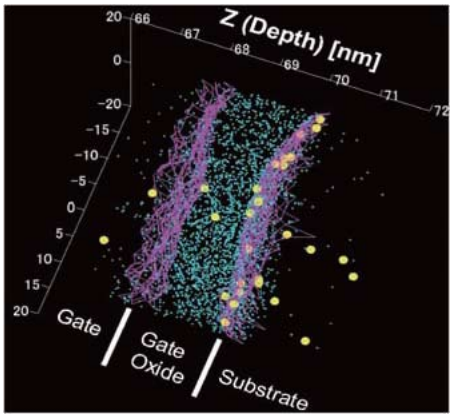

Fig. 3 Enlarged view of the 3D elemental map around the gate oxide. As (yellow) and O (blue).

References

[1] K.Inoue, F.Yano, A.Nishida, T.Tsunomura, T.Toyama, Y.Nagai, M.Hasegawa: App. Phys. Lett. **92** (2008) 103506.

Key Words

Laser 3D Atom Probe, Interface Segregation

Contact to

Yasuyoshi Nagai (Irradiation Effects in Nuclear and Their Related Materials Division)

e-mail: nagai@imr.tohoku.ac.jp

Superconductivity Induced by Electric Field

New superconductors have so far been discovered by chemical doping in an insulator. We demonstrated for the first time that an electrrostatic charge carrier doping can induce superconductivity. It was performed by the application of a few volts to a $SrTiO_3$ through a self-organized electric double layer. This method will provide a new pathway for the future search of novel high-temperature superconductors.

Chemical substitution of impurity elements provides mobile charge carriers to a solid and makes it conductive. Many insulators can be converted to exhibit metallic conduction by increasing charge carrier density and some of them show superconductivity with zero-resistance at low temperature above certain charge carrier density, as shown in the upper panel of Fig. 1. This method is called "chemical doping" and has been widely used to search for new superconducting materials, such as high temperature cuprates, fullerene superconductors, and recently discovered iron-based superconductors. Electric field-effect is another promising candidate method for modifying the charge carrier density in a solid. By fabricating a field-effect transistor, one can electrically modulate charge carrier density in a semiconductor channel by the application of a gate bias voltage through a gate isnulator. So far, however, field-effect modulation of charge carrier density is far insufficient for inducing superconducting state in any insulating material. This is due to a low breakdown field in the gate insulator. Recently, we have developed a new field-effect transistor, "electric double layer transistor" with oxide semiconductor channel, which can induce much higher charge carrier density than that in conventional field-effect transistors [1]. In an electric double layer transistor, a semiconductor channel and a gate metal electrode are immersed in an electrolyte solution that works as the gate insulator, as shown in the bottom panel of Fig. 1. By the application of a gate bias voltage, cations move towards the interface between the electrolyte and the channel, and then an electric double layer is formed at the interface. Due to a high breakdown field of the electric double layer and very thin (1nm) separation formed in a self-organized manner between the cations and surface, high density charge carriers can be accumulated on the channel.

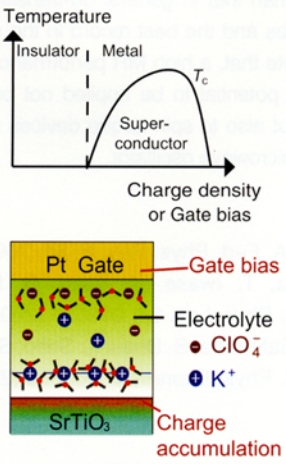

Fig. 1 (Upper panel) Schematic phase diagram of $SrTiO_3$. Many insulators, such as Si and high-T_c cuprates, show similar phase diagram. (Bottom panel) Schematic diagram for an electric double layer transistor. An electric double layer is formed at the interface between a $SrTiO_3$ channel and an electrolyte with K^+ cations, thereby high density charges are accumulated.

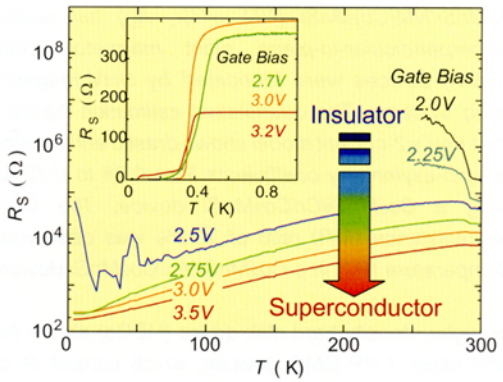

Fig. 2 Temperature (T) dependence of sheet resistance (Rs) for the $SrTiO_3$ channel of the electric double layer transistor under various gate biases. For gate biases above 2.5 V, good metallic conduction took place even at low temperature. Inset shows Rs-T curves at low temperature. Clear superconducting transition with zero resistance was seen at a critical temperature Tc = 0.4 K.

The first example of electric field induced superconductivity was demonstrated as followings [2]. We fabricated an electric double layer transistor device with a non-doped $SrTiO_3$ single crystal as a semiconductor channel and with polyethylene oxide solution containing $KClO_4$ as an organic electrolyte. Application of gate bias of several volts induces high density charges up to $10^{14}cm^{-2}$, which is far above the maximum value in a conventional Si field-effect transistor. Charge carrier density is monotonically increased with increasing gate bias (V_G), and the channel shows good metallic conduction down to 2 K for V_G above 2.5 V, as shown in Fig. 2. At low temperature, the metallic channel shows zero resistance state for various gate biases, as shown in the inset of Fig. 2. From a subband calculation, it appears that the charge carrier density of the channel is modulated from zero to $10^{20}cm^{-3}$. This charge carrier density is expected to be sufficient for inducing superconducting state in many insulator materials. In addition, this method can provide conductivity to many insulators where chemical doping does not work. This electrical method will considerably extend the candidate materials for possible new superconductors to many unprecedented insulator materials.

References

[1] H. Shimotani, H. Asanuma, A. Tsukazaki, A. Ohtomo, M. Kawasaki and Y. Iwasa, Appl. Phys. Lett. 91, 082106 (2007).
[2] K. Ueno, S. Nakamura, H. Shimotani, A. Ohtomo, N. Kimura, T. Nojima, H. Aoki, Y. Iwasa and M. Kawasaki, Nature Mater. 7, 855 (2008).

Key Words

Superconductor, Oxide Electronics, Field Effect Transistor

Contact to
Masashi Kawasaki (Superstructured Thin Film Chemistry Division)
e-mail: kawasaki@imr.tohoku.ac.jp

Giant magnetoresistance in Co_2MnSi-Based Fully-Epitaxial Current-Perpendicular-to-Plane Magnetoresistive Devices

Co_2MnSi/NM/Co_2MnSi (NM = Cr, Ag) fully-epitaxial current-perpendicular-to-plane giant magnetoresistance (CPP-GMR) devices were fabricated by UHV magnetron sputtering systems. The quantitative estimation based on Valet and Fert's 2-current model shows drastic enhancement of bulk spin-asymmetry coefficients from 0.38 to 0.72 after annealing a Co_2MnSi/Cr/Co_2MnSi device. The largest magnetoresistance (MR) ratio of 28.8% was observed at room temperature (RT) in a Co_2MnSi/Ag/Co_2MnSi device.

For higher-density hard disk drives (HDDs) above the 1 Tbit/inch^2 class, CPP-GMR devices, which consist of only metallic layers, attract much attention as next generation magnetic reading heads because these devices are predicted to exhibit a small *RA* suitable for high-speed reading. However, the biggest drawback of CPP-GMR is a small MR ratio compared to those of MgO-MTJs. Hence, in recent years, half-metallic materials are often employed as ferromagnetic electrodes in order to enhance the MR ratio in CPP-GMR. Half-metallic materials have an energy band gap at the Fermi level only in the up or down spin-channel. Therefore, the large spin-asymmetry of electron scattering, i.e., large difference between electrical resistances for the up and down spin-electrons, is anticipated. In a number of half-metal candidates, Co-based full-Heusler alloys, such as Co_2MnSi (CMS), are promising because previous studies on magnetic tunnel junctions have experimentally confirmed their half-metallicity. We fabricated CPP-GMR devices with fully-epitaxial CMS /Cr or Ag/ CMS structures and investigated the magneto-transport properties systematically.

All films were prepared by UHV-compatible magnetron sputtering and patterned into pillars with sizes of 50 x 100nm^2 to 300 x 600nm^2 by a micro-fabrication process. MR properties were investigated by a standard dc 4-probe method.

For the quantitative estimation of spin-asymmetries of electron scattering in CMS/Cr/CMS devices, we investigated the CMS thickness dependence of resistance change area product (ΔRA) before and after annealing (Fig.1). As a result of fitting based on Valet and Fert's 2 current-model [1], bulk and interfacial spin-asymmetries, β and γ, which are defined as $(\rho_\uparrow - \rho_\downarrow)/(\rho_\uparrow + \rho_\downarrow)$, were evaluated to 0.38 and 0.47, respectively, in the as-deposited state. Interestingly, β was dramatically enhanced to 0.72 by annealing at 350°C. This result implies that half-metallicity was improved by promoting $L2_1$-chemical order in CMS electrodes [2]. Furthermore, β increased to 0.92 at 6 K, which means nearly ideal half-metallicity in the CMS electrodes.

In CMS/Ag/CMS devices, we also investigated the CMS thickness dependence of ΔRA and MR ratio. It was found that γ was large for CMS/Ag ($\gamma = 0.74$) compared with that for CMS/Cr, which is a very important advantage for applying a CMS/Ag/CMS device to a magnetic reading head since there is a limitation of the total film thickness caused by the read gap length in a recording media. Another big advantage of the Ag interlayer is a small solubility to CMS, which enables to increase annealing temperature to 500°C and enhances the degree of $L2_1$-chemical order. Large β and γ results in a high MR ratio of 28.8% at RT in a CMS/Ag/CMS device (Fig. 2) [3]. This MR ratio at RT is almost 10 times larger than that in general 3*d*-transition metal-based CPP-GMR devices and the best record in the reports of CPP-GMR to date. Note that, a high MR performance owing to half-metallicity has a potential to be applied not only to magnetic reading heads but also to spin-torque devices such as a spin-torque induced microwave oscillator.

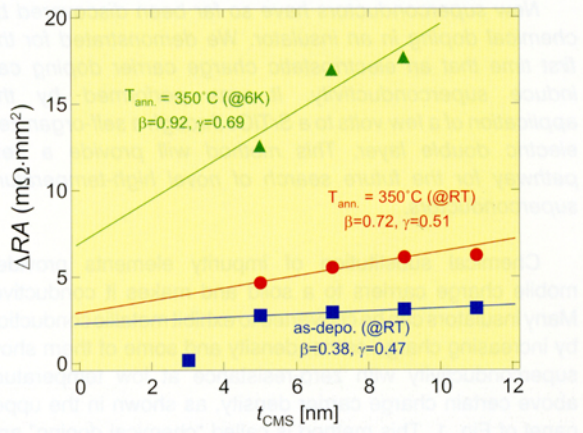

Fig. 1 CMS thickness dependence of ΔRA for a CMS/Cr/CMS CPP-GMR device in the as-deposited state and after annealing at 350°C. The lines show fitting results by Valet and Fert's model.

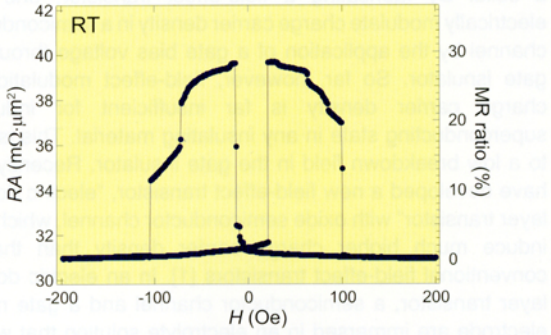

Fig. 2 Applied magnetic field dependence of *RA* (left) and MR ratio (right) at RT in a CMS/Ag/CMS CPP-GMR device.

References

[1] T. Valet and A. Fert, Phys. Rev. B, **48**, 7099 (1993).
[2] Y. Sakuraba, T. Iwase, K. Saito, S. Mitani, and K. Takanashi, Appl. Phys. Lett. **94**, 012511 (2009).
[3] T. Iwase, Y. Sakuraba, S. Bosu, K. Saito, S. Mitani, and K. Takanashi. Appl. Phys. Express **2**, 063003 (2009).

Key Words

Spintronics, Half Metal, CPP-GMR

Contact to
Koki Takanashi (Magnetic Materials Division)
e-mail: koki@imr.tohoku.ac.jp

Spin Glass Behavior in NMAD Uranium Compound U_2CuSi_3

Ternary nonmagnetic atom disorder (NMAD) uranium compound U_2CuSi_3 is confirmed to crystallize in the tetragonal α-$ThSi_2$-type structure after annealed at 800℃ for 240h. Ac susceptibility measurements reveal an evident spin glass transition for this compound at a static spin freezing temperature T_S=18.3K. The presence of frustrated magnetic interactions in U_2CuSi_3 is discussed in a "magnetic cluster model".

Ternary uranium compounds U_2XSi_3 (*X*=transition metal) have attracted much interest in the last decade. The considerable changes of magnetic properties in these systems have been demonstrated to relate with the character of the *X* atom and the arrangement of non-magnetic atoms (*X* and Si) in *X*-Si network. For examples, Spin glass (SG) behavior, paramagnetic properties and ferromagnetic cluster glass behavior have been observed for the compounds with *X*= Pd, Rh and Fe, which crystallize in the hexagonal structure with *perfectly* disordered, *partially* disordered and *perfect* order arrangement of *X* and Si atoms, respectively. For U_2CuSi_3, it is known as a special and interesting case in the family of compounds U_2XSi_3 relevant to its controversial magnetic properties and crystal structures. U_2CuSi_3 was first reported to crystallize in the tetragonal α-$ThSi_2$-type structure exhibiting *re-entrant SG* behavior, and in the later literature it was considered as a ferromagnetic material with the hexagonal AlB_2-type structure.

We have systematically measured the basic physical properties of U_2CuSi_3 on a well-annealed polycrystalline sample, which was confirmed to crystallize in the tetragonal α-$ThSi_2$-type structure after annealed at 800°C for 240 h [1]. Figure 1 presents the low temperature dc susceptibility ($\chi=M/H$) data measured in a field of H=100 Oe. With decreasing temperature, the χ_{ZFC} (T) curve shows a sharp peak near T_f~18.9 K, suggesting a certain kind of magnetic phase transition at this temperature. However, no peak is observed in the χ_{FC} curve and evident magnetic irreversibility manifesting as the bifurcation between the χ_{ZFC} and χ_{FC} curves appears below a temperature T_{ir}, similar to that usually observed in SG materials. In addition, no any indication of a magnetic phase transition into a long-range order around T_f (~18.9 K) can be observed in both the specific heat C (T) (inset (a) of Fig. 1) and the electrical resistivity $\rho(T)$ (inset (b) of Fig. 1) curves. These results suggest the absence of long-range spatial magnetic order in the vicinity of T_f.

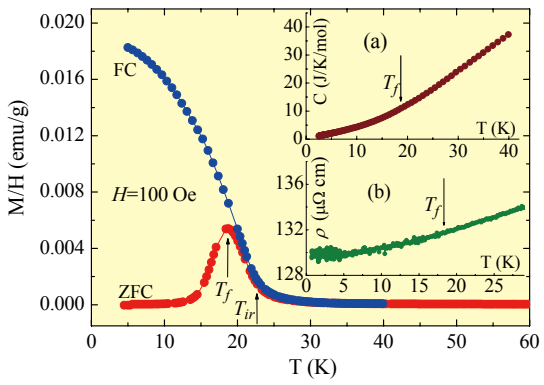

Fig. 1 Temperature dependences of field-cooled (FC) and zero-field-cooled (ZFC) dc susceptibility ($X=M/H$) of U_2CuSi_3 in an applied field of 100 Oe. The insets (a) and (b) show the temperature dependences of specific heat and electrical resistivity, respectively, for the U_2CuSi_3 sample.

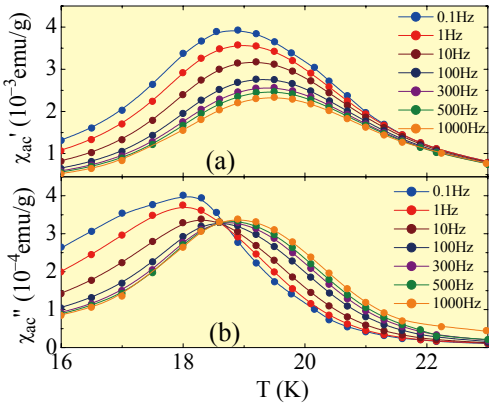

Fig. 2 Real (a) and imaginary (b) components of the ac susceptibility of U_2CuSi_3 vs. temperature at various frequencies.

Figure 2 shows the in-phase $\chi'_{ac}(T,\omega)$ as well as the out-of-phase $\chi''_{ac}(T,\omega)$ components of the ac susceptibility versus temperature between 16 and 23 K. Both the χ'_{ac} and χ''_{ac} curves exhibit a characteristic pronounced maximum with amplitude and position depending on the frequency ω of the applied ac magnetic field. As ω increases, the peak position in χ'_{ac} and χ''_{ac} shifts to higher temperatures. Such a feature can be considered as the most striking evidence for SG state in U_2CuSi_3. The initial frequency shift of the peak position is determined to be $\delta T_f=\Delta T_f/(T_f\Delta\log\omega)=0.009$. This value is comparable to the typical values reported for canonical SG systems. From the dynamical analyses of the ac susceptibility data, the static spin freezing temperature T_S, critical exponent $z\nu$ and activation energy E_a are determined to be 18.3 K, 8.1 and 3.1 k_BT_S, respectively.

It is well known that "randomness" and "frustration" are the necessary conditions for SG state. To understand the existence of frustrated magnetic interactions in U_2CuSi_3, we considered that statistical arrangement of nonmagnetic Cu and Si atoms could destroy long-range magnetic correlation between U atoms in U_2CuSi_3 and lead to the formation of individual spins or finite-size granules with net magnetic moments (magnetic clusters). These clusters should also randomly distribute in the sample and interact on each other at low temperature causing the formation of frustrated magnetic moments. Below a freezing temperature T_f, these frustrated magnetic moments could be frozen-in along random directions to form a spin glass state similar to what happen in amorphous or diluted metallic SG materials.

References

[1] D. X. Li, S. Nimori, T. Yamamura and Y. Shiokawa, J. Appl. Phys. **103**, 07B715 (2008).

Key Words

Spin Glass, Susceptibility, Frustrated Magnetic Interactions

Contact to
Dexin Li (Radiochemistry of Metals Division)
e-mail: dxli@imr.tohoku.ac.jp

Room Temperature Coulomb Oscillation of a Proton Dot in Ni-Nb-Zr-H Glassy Alloys with Nanofarad Capacitanc

A dc current-induced voltage oscillation was observed at room temperature in $(Ni_{36}Nb_{24}Zr_{40})_{90.1}H_{9.9}$ glassy alloy ribbons of about 1-mm width and 30-μm thickness and an electrode distance of 20 mm [1]. The I-V characteristic provided evidence of the Coulomb staircase at ~300 K, suggesting the existence of macroscopic proton dot tunneling along the Zr(Nb)-H-□-H-Zr(Nb) atomic bond array, where □ is the vacancy barrier among clusters. The frequency decreased remarkably with increasing capacitance (C) and resistance (R) at room temperature. Thus the $(Ni_{36}Nb_{24}Zr_{40})_{90.1}H_{9.9}$ glassy alloy can be regarded as a dc/ac converting device with a large number of nF capacitance.

Quantum dot tunnelling is one of the topics currently attracting a great deal of interest in the field of physics. If room-temperature macroscopic quantum dot tunnelling is realized, it will lead to epoch-making developments in the manufacture of electronic devices. Although the challenges in realizing quantum dot tunnelling at room temperature have been carried out by various research groups, no research work has achieved a success for the SETs, on the millimeter size, as far as we know. We investigate an effect of Zr content on Coulomb oscillation in the millimeter sized Ni-Nb-Zr-H glassy alloys in anticipation of room-temperature Coulomb oscillation.

We measured *I-V* characteristics at temperatures ranging from 8 K to 412 K, because a stepwise increase of the current *I* upon increasing the applied voltage *V* is expected for tunnel barriers [2, 3]. Fig.1 shows a typical Coulomb staircase, indicative of quantum dot tunnelling, as can be seen from "Coulomb gap" shown by a hyperbolic curve in *I-R* characteristics at 300 K (insert). The width ΔV = 0.10 mV of the current plateaus is a direct measure of the charging energy: $e\Delta V = e^2/C$, from which we deduce the total capacitance C = 1.60 fF. To obtain information on the tunnel barrier height and width, the conductivity was plotted as a function of the inverse temperature ($1/T$), the Arrhenius plot in Fig.1, and measured for the fixed E =0.10 mV. It can be seen that there are two distinct temperature regions. At a temperature below ~300 K, the current is almost constant, whereas it increases noticeably with increasing temperature. The former behavior is that of tunnelling, whereas the latter is an activation process which arises from the thermionic emission over the tunnel barrier.

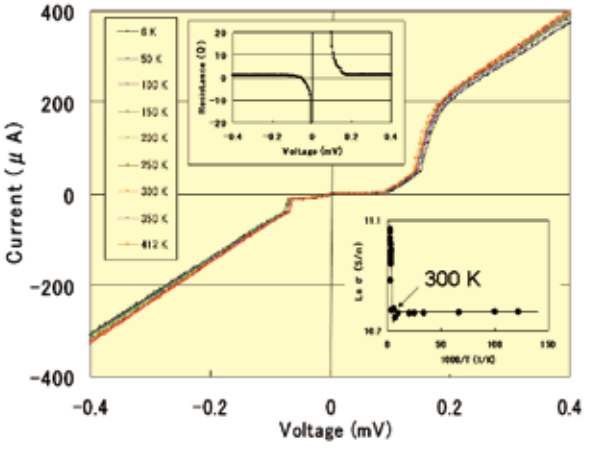

Fig. 1 *I-V* characteristics at temperatures ranging for $(Ni_{36}Nb_{24}Zr_{40})_{90.1}H_{9.9}$ glassy alloy at 8, 50, 100, 150, 200, 250, 300, 350 and 412 K. Insert: the voltage-controlled *I-R* characteristics at 300 K. Arrhenius plot of the conductivity as a function of the inverse temperature.

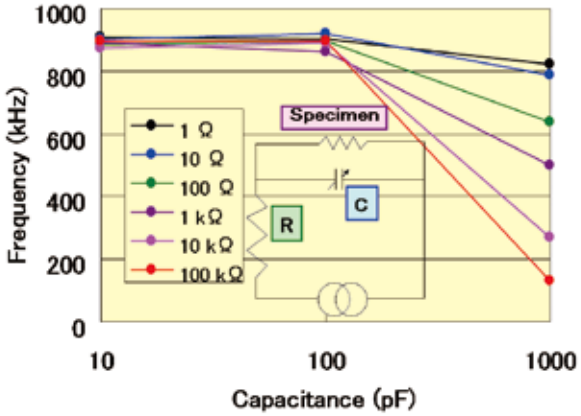

Fig. 2 Capacitance dependence of frequency for various resistances in $(Ni_{36}Nb_{24}Zr_{40})_{90.1}H_{9.9}$ glassy alloy. Insert: Oscillation circuit used in study. R, C and E are resistance, capacitance and dc voltage source, respectively.

Since the alloy $(Ni_{36}Nb_{24}Zr_{40})_{90.1}H_{9.9}$ causes dc current-induced ac oscillation at room temperature, we concluded this study by investigating the RC effect on the oscillation in the dc/ac circuit. The capacitance dependence of frequency for various resistances at room temperature is shown in Fig.2, along with the frequency circuit. In the capacitance region over 100pF, the frequency decreases remarkably with increasing resistance from 900kHz.

References

[1] M.Fukuhara and A.Inoue, J.Appl.Phys., **105**, 063715 (2008).

[2] M.Fukuhara A.Kawashima, S.Yamaura and A.Inoue, Appl.Phys.Lett., **90**, 203111(2007).

[3] M.Fukuhara and A.Inoue, Europhus.Lett., **83**, 36002 (2008).

Key Words

Nano Quantum Dot Tunnelling, Electronic Device

Contact to

Mikio Fukuhara (Research and Development Project on Advanced Metallic Glasses, Inorganic Materials and Joining Technology)

e-mail: fukuhara@imr.tohoku.ac.jp